DISTILLATION TRAY STRUCTURAL
PARAMETER STUDY: PHASE I

J. Ronald Winter
Senior Engineering Mechanist
Engineering Division
Tennessee Eastman Company
Kingsport, Tennessee

ABSTRACT

The major purifications process used by the petro/chemical industries is called "distillation." The associated pressure vessels are referred to as distillation columns. These vessels have two basic types of internals: distillation trays and packing. Some special columns have both a packed section and a trayed section. This paper deals with the structural (static and dynamic) analysis of distillation trays within a column. Distillation trays are basically orthogonally stiffened circular plates with perforations in a major portion of the surface. Structural failures of such trays are often attributed to vibration associated with either resonant or forced response. The situations where resonance has been encountered has led to immediate structural failures. These resonant conditions are attributed to the presence of a process pulsation with a frequency within the half-power band width of the first or second major tray structural natural frequency. The other major class of failures are due to fatigue associated with forced response. In addition, occasional tray structural failures have been encountered as a result of sudden large pressure surges usually associated with rapid vaporization of a liquid (flashing), a minor explosion or a sudden loss of vacuum. These latter failures will be briefly discussed in this paper. It should also be noted that corrosion is a common problem that often leads to structural failures and/or a decrease in tray processing efficiency.

The purpose of this study is to identify the structural parameters (plate thickness, liquid level, beam size [moment of inertia], number of beams, tray diameter, etc.) that affect the structural integrity of distillation trays. Once the sensitivity of the trays dynamic response to these parameters has been established, the designer will be able to use this information to prepare more accurate specifications for the construction of new trays. This will result in a reduction in the failure rate which in turn will lead to lower maintenance cost and greater equipment utilization.

LIMITATIONS

This is a report on Phase I of a two phase analysis. It is applicable to trays with diameters ranging from 10 feet to 15 feet and having a single main beam in addition to smaller minor beams. The results are mainly applicable to cross-flow type distillation trays of either the sieve or valve configurations. See Figures 1 and 6, and Appendices I and II. In addition, these results would only apply to trays made of certain metals such as carbon steel, stainless steel, Hastelloys, monels, etc. They would not be applicable to trays made of titanium, copper, aluminum, plastic, etc. Phase II of this study will deal with trays of the same type that have diameters ranging from 3 feet to 10 feet but that do not have a main beam. NOTE: A typical Engineering drawing of a smaller diameter valve tray is shown in Appendix I.
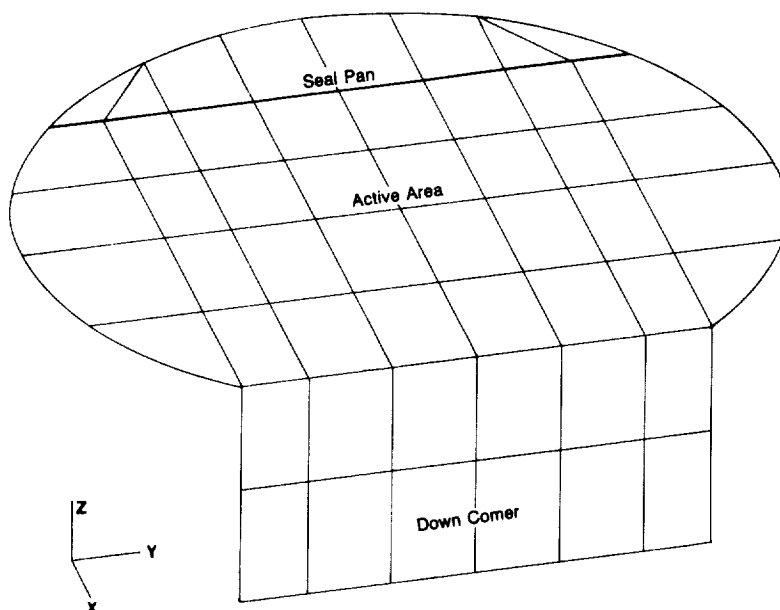

Figure 1: Configuration of a Typical Cross Flow Distillation Tray

ENGLISH TO METRIC CONVERSIONS

All data presented in this report are in English units. Use the table below to convert items to SI (metric) units.

To Convert From	To	Multiply By
Inches	Millimeters	25.4
Square Inches	Square Millimeters	645.2
Inches^4	Centimeters^4	41.62
Feet	Meters	0.3048
Pounds Mass	Kilograms	0.4536
Pounds Force	Newton	4.448
Pounds Per Square Inch	Pascal	6,894.7
Pounds Per Square Foot	Pascal	47.88
Pounds Per Cubic Inch	Kg Per Cubic Meter	2,678

PROCESS OPERATION

The typical geometric layout of trays inside a column is shown in Figure 2. In most situations a pool of liquid chemicals at the bottom of the column is boiled by use of a heat exchanger (reboiler). This is shown in Figure 3. The resulting vapor moves up the column through the perforated plates. At the same time a liquid consisting of two or more chemicals is added at some point around the middle of the column. A relatively pure liquid stream is also added to the top tray of the column. This is referred to as the reflux. The liquid flows across the trays moving down the column, as shown in Figure 4. The resulting heat transfer from tray to tray causes the liquid with the lowest boiling point to vaporize and move up the column while the higher boiling point liquid(s) flows counter current down the column. Purification is thus achieved by the separation of the components with different boiling points.
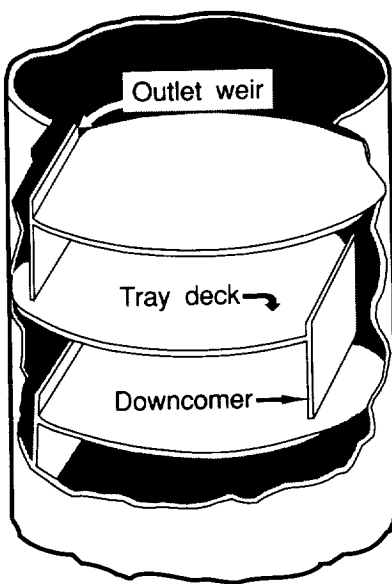

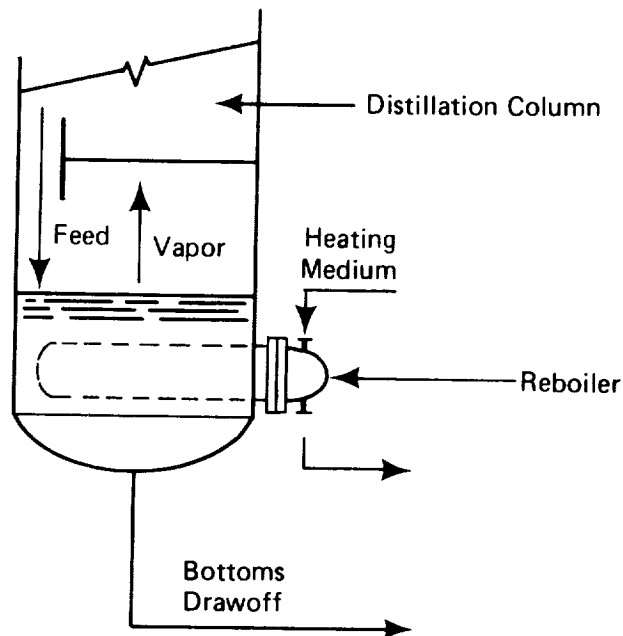Figure 2: Tray Locations Inside of a Column

Figure 3:   General Configuration of the Bottom Section
of a Distillation Column

As shown in Figure 4, the liquid flows diagonally across the tray
while the vapor flows through the perforations perpendicular to
the liquid flow. As stated previously, the liquid-vapor
interactions throughout the column serve to separate the low
boiling and high boiling liquids. The result is a vapor flow
from the top of the column with a high concentration of the low
boiling liquid while the liquid in the base consists of a high
concentration of the high boiling liquid(s).

The vapor-liquid interaction in the column can be quite violent
depending on the vapor velocity through the tray perforations
versus the liquid depth on the tray. This generally produces a
liquid froth in a portion of the space between trays. This
interaction also produces natural pulsations with the amplitude
being sensitive to the ratio of the liquid depth to the vapor
velocity. These pulsations are often referred to as
auto-pulsations.

Such pulsations (auto-pulsations) produce tray oscillations, the
most dangerous of which is a resonant or near resonant condition.
This occurs when the auto-pulsation frequency, f_A, is within the
half-power bandwidth of the tray first or second natural
frequencies, ω_1 and ω_2. This can lead to immediate destruction
of the affected trays. One such situation will be discussed in
this paper. The other situation involving auto-pulsations
produces large fluctuations in pressure across individual trays.
This results in forced response which can lead to fatigue
failures. Examples of this more prevalent type failure mode will
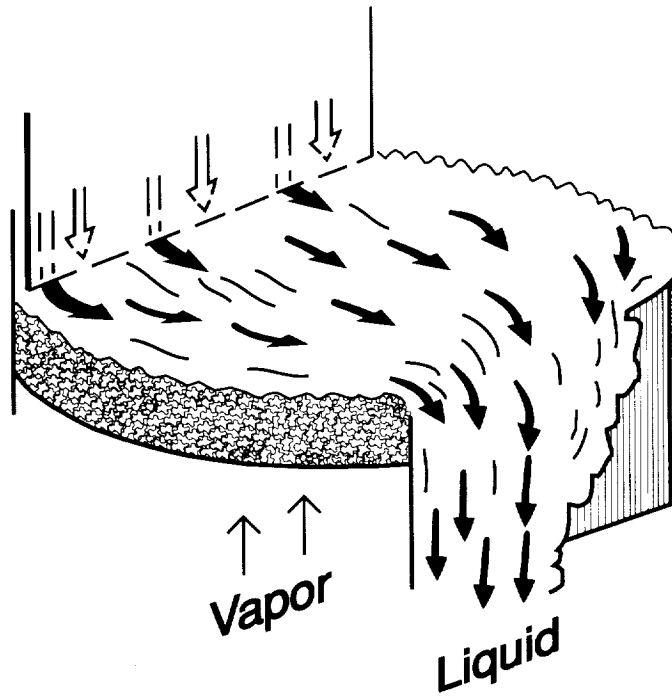also be discussed.

90

Figure 4: Liquid and Vapor Flow on a Tray

DYNAMIC ANALYSIS

The major emphasis of this study was modal analysis of distillation trays with the major goal to determine the structural parameters that have the most significant effect on the first and second tray structural natural frequencies. This would give the designer the ability to more effectively change the tray design to prevent a resonant, or near resonant condition, or to decrease the amplitude of the trays forced response to auto-pulsation.

STATIC ANALYSIS

The static analyses were limited to determining the maximum deflection of the center portion of the tray due to normal design loads. Large deflections (δ > 0.125") at the center of a tray leads to significant variations in liquid depth across the trays which adversely affects tray performance (efficiency). The design loads for the active tray area vary from 25 psf to 45 psf depending on the tray diameter and the process. *A design load of 64 psf is usually used for the seal pan.

One can use a combination of the tray design load and the allowable tray deflection as a means to control a tray's dynamic response. This is often necessary for use in specifications since most tray manufacturers do not have the personnel to perform dynamic finite element analyses.

As described previously, auto-pulsation is associated with vapor-liquid interaction on a tray deck as the liquid flows across the tray and the vapor passes through the perforations in the tray deck. As of this date, no one has developed a math model that adequately describes this phenomena. However, some imperical models do exist. Better imperical models could be developed if more data were available for the various combinations of tray diameter, liquid depth, open area (number and size perforations), tray spacing and flow rates. Fortunately, we do have enough data to establish some general trends. Relative to auto-pulsation the "**available**" data "**indicates**" the following trends:

(1) The auto-pulsation frequency, f_A, increases with increasing tray (column) diameter. (See Figure 5)

(2) f_A increases with increasing hole diameter or number of holes; i.e., with increasing open area for vapor flow.

(3) f_A decreases with increased tray spacing; i.e., distance between trays.

(4) f_A increases somewhat as the outlet weir height (liquid depth) increases.

The graph of f_A vs diameter in Figure 5 is shown as a broad band since f_A is also sensitive to the variables discussed in Items 2, 3 and 4 above. In addition f_A is somewhat sensitive to tray performance associated with proper tray installation, operating conditions, stability of the heat exchange system, etc.
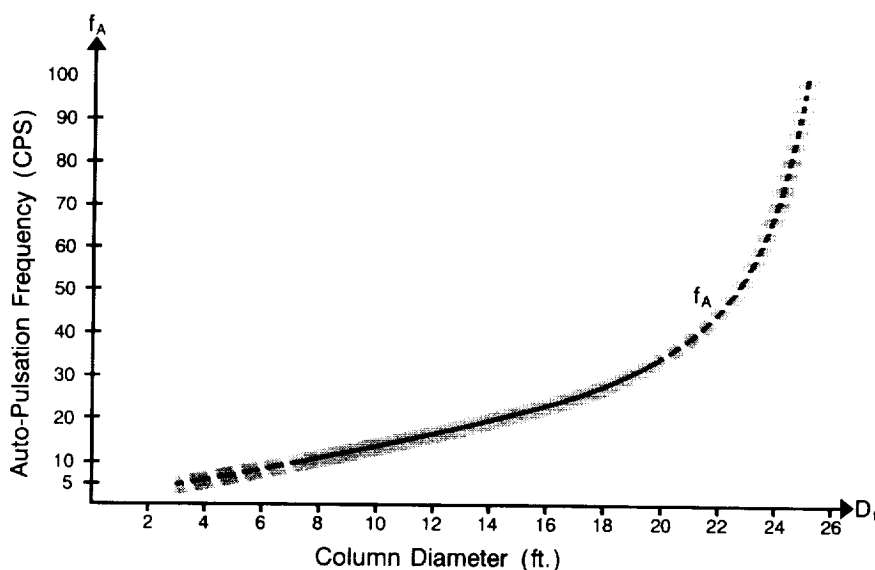

Figure 5:   Auto-pulsation Frequency, f_A, Versus Tray/Column Diameter

Tests have also shown that a low frequency pulsation exists that appears to be independent of tray diameter. In some publications this has been referred to as a "swashing" frequency[3,4,5,6]. It involves a wave action across the tray, perpendicular to the liquid flow. In some discussions, engineers refer to it as a standing wave whose frequency is, for the most part, independent of tray diameter. The frequency is generally less than 5 cps.

STRUCTURAL PARAMETER STUDY

The tray structural parameters considered in the static and dynamic analysis of the trays are:

(1) Tray diameter, (D_t): 10 feet to 15 feet.

(2) Tray (plate) thickness, (t_p): 11, 12, 14 gauge.

(3) Minor beams (tray turn downs) moment of inertia, $(I_S = I_{XX})$.

(4) Major beam moment of inertia, $(I_B = I_{YY})$.

(5) Liquid depth on the tray, h_L.

In addition, one must make special corrections to attain the proper mass in the model. First, the thickness of the tray must be reduced to reflect the perforations. If it is a valve tray, then the weight of the valves must be added back into the model as non-structural mass. The effective liquid depth* on the active tray area must be added as non-structural mass. In addition, the higher liquid depth in the seal pan area must be added into the model as non-structural mass.
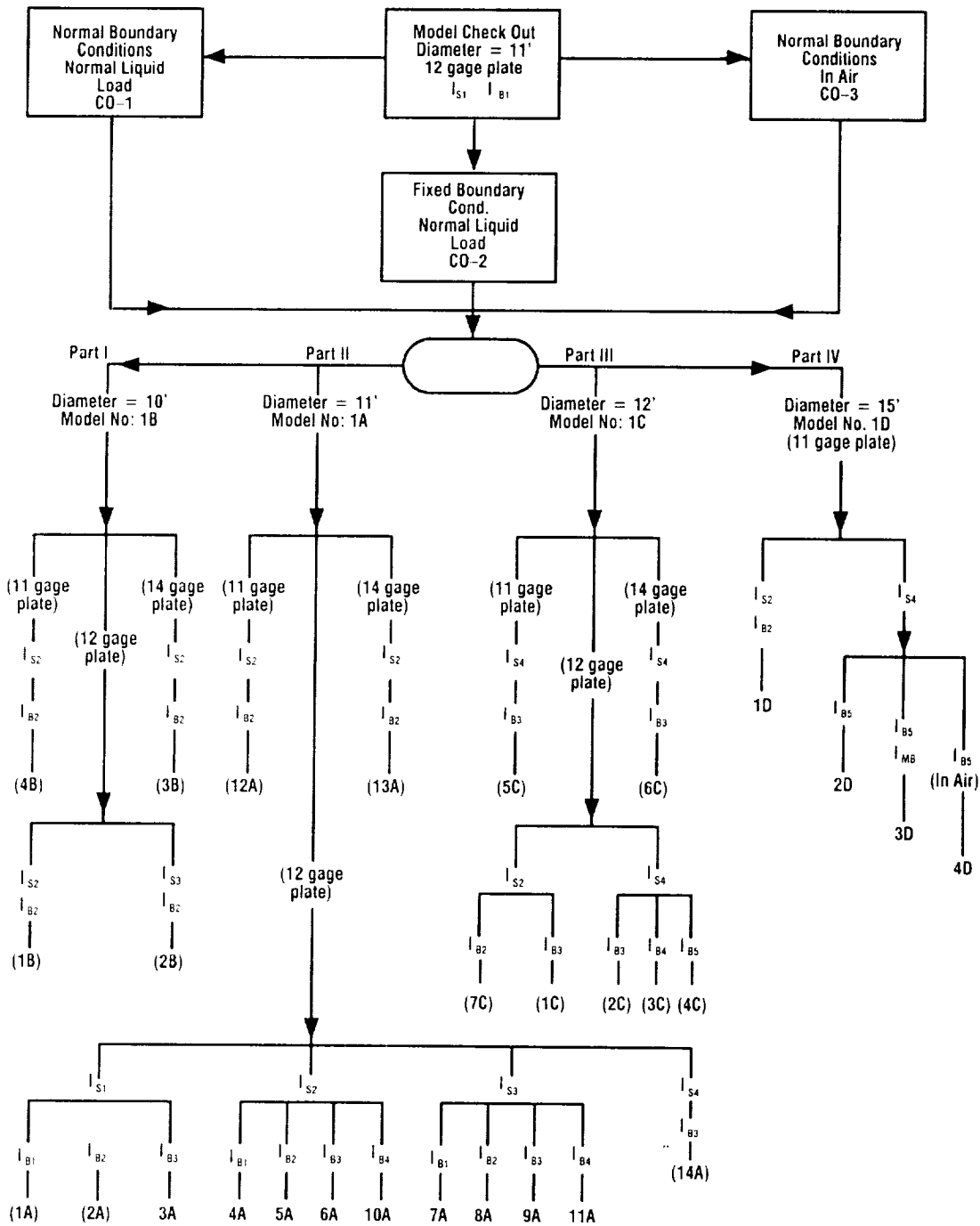
The number of models developed and the parameters involved are shown in the flow chart on the next page. Each basic model is indicated by a number-letter combination such as 5A. Run 5A involves a 11 ft diameter, 12 gauge tray with minor beam I_{S2} and major beam I_{B2}. This particular model, as well as the other ones, were ran with different liquid depths. In addition to the dynamic (modal) analysis a static analysis was performed on each model. Typical boundary conditions as well as a static load set are presented in Appendix VI.

EXAMPLE ANALYSIS OF A TRAY THAT ENCOUNTERED RESONANCE

This particular column has a diameter of 11 ft. The column contained cross-flow valve trays in the upper half of the vessel and split flow valve trays in the bottom half. Only the more flexible cross flow valve trays as shown in Figure 6 encountered problems. Split flow trays are inherently stiffer than the same diameter cross flow trays provided both are designed for the same loading.

*Due to the vapor liquid interaction the effective liquid depth (liquid mass associated with the tray) will differ from the actual undisturbed liquid depth.

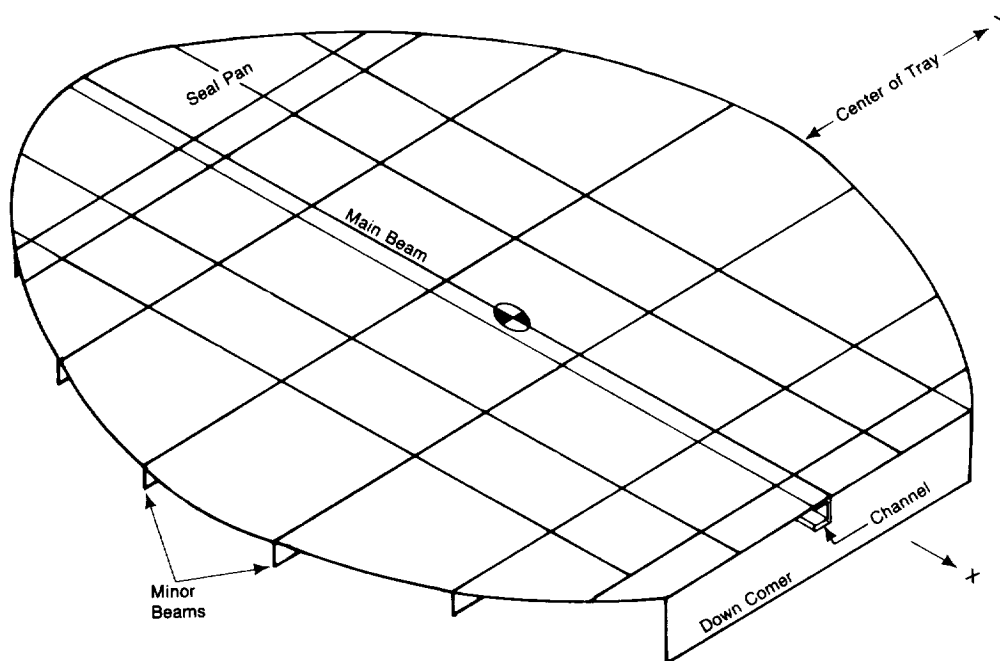# DISTILLATION TRAY STRUCTURAL PARAMETER STUDY: PHASE I

Normal Boundary
Conditions
Normal Liquid
Load
CO-1

Model Check Out
Diameter = 11'
12 gage plate
I_{S1} I_{B1}

Normal Boundary
Conditions
In Air
CO-3

Fixed Boundary
Cond.
Normal Liquid
Load
CO-2

Part I
Diameter = 10'
Model No: 1B

Part II
Diameter = 11'
Model No: 1A

Part III
Diameter = 12'
Model No: 1C

Part IV
Diameter = 15'
Model No. 1D
(11 gage plate)

(11 gage plate) I_{S2} (12 gage plate)   (14 gage plate) I_{S2}
I_{B2} I_{B2}
(4B)   (3B)

(11 gage plate) I_{S2} (14 gage plate) I_{S2}
I_{B2} I_{B2}
(12A)   (13A)

(11 gage plate) I_{S4} (12 gage plate)   (14 gage plate) I_{S4}
I_{B3} I_{B3}
(5C)   (6C)

I_{S2} I_{B2}
1D

I_{S4}
I_{B5} I_{MB} I_{B5}
2D   3D   (In Air)
4D

I_{S2} I_{S3}
I_{B2} I_{B2}
(1B)   (2B)

(12 gage plate)

I_{S2} I_{S4}
I_{B2} I_{B3} I_{B3} I_{B4} I_{B5}
(7C)   (1C)   (2C)   (3C)   (4C)

I_{S1} I_{S2} I_{S3} I_{S4}
I_{B1} I_{B2} I_{B3} I_{B1} I_{B2} I_{B3} I_{B4} I_{B1} I_{B2} I_{B3} I_{B4} I_{B3}
(1A)   (2A)   3A   4A   5A   6A   10A   7A   8A   9A   11A   (14A)

94

Figure 6: Original Cross Flow Tray

Two finite element codes were used in this analysis:

STRAP3:   A code developed by The Eastman Kodak Company for
           internal use before the release of numerous other
           finite element codes.

NASTRAN: NASA structural Analysis Code[1,2]. Developed
           by NASA at Goddard Space Flight Center and
           released to the general public in 1970. The
           latest versions are now available for lease from
           COSMIC at the University of Georgia, Athens,
           Georgia.

Structural/Model Details

The original tray configuration is shown in Figure 6. There are
two structural details that have a significant affect on the tray
modal response.

(1)   The minor beams are straight; i.e., they are not angles
       or channels which are more commonly used today.

(2)   The main beam is a channel instead of an I-beam. Thus
       to get the correct first mode shape (modal response)
       one must correct for the shear center. This was done.
       The applicable model in the flow chart is 12A. The
       checkout model also applies.

Tray Failure Details

During initial start-up of the column, all process operations were proceeding normally until the tray operation was at about 25% of its capacity. At this point the overall column efficiency began to drop dramatically as the flow-rates increased. The unit was shut down in an effort to determine the cause of the unexpected loss in capacity. Internal inspection of the column revealed:

(1) Cracks at the turn down (minor beams) on the tray decks. See Figure 7.

(2) Cracks in the main beam (channel). See Figure 8.

(3) Damaged valves and tray hardware. See Figures 9 and 10.

(4) Valves missing on the tray deck on one side of the channel; the side opposite the open U. See Figures 7, 11 and 12.

(5) The vessel wall also cracked where the main beam was attached to the wall.
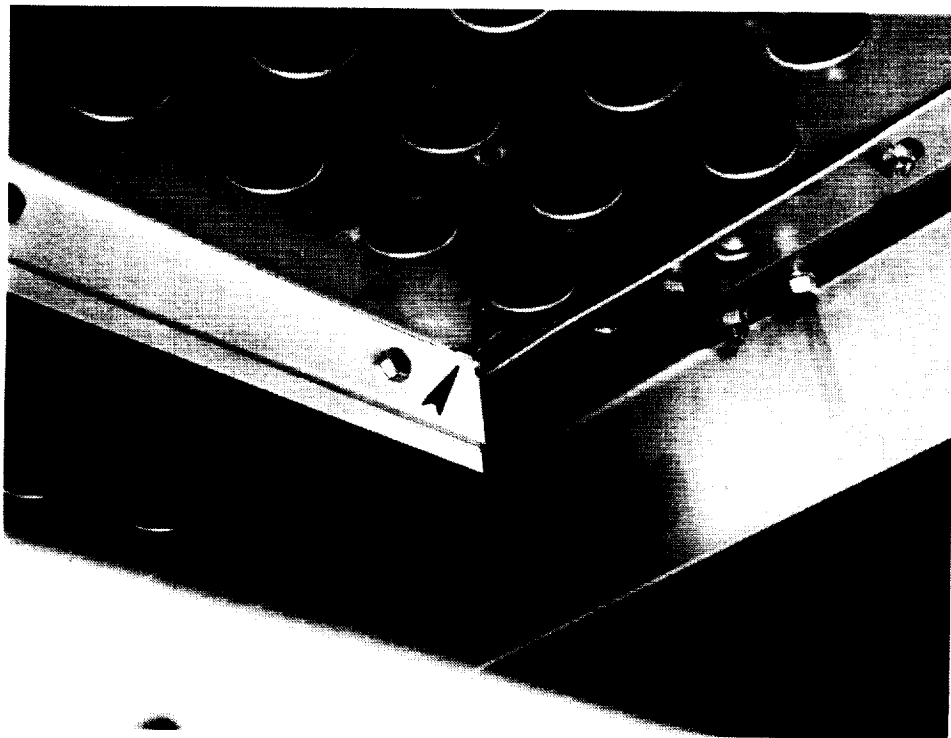
Figure 7: Tray Deck and Minor Beam Cracking
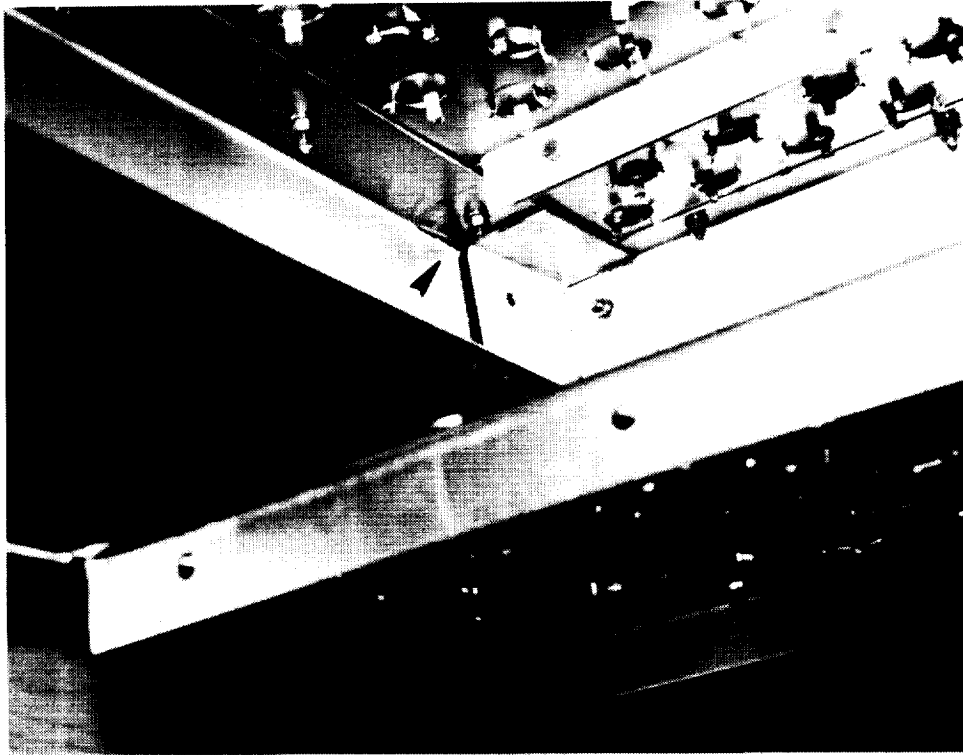
Figure 8:   Main Beam Cracking

As shown in Figure 9, some of the legs are broken off the valves
due to the dynamic action.   Close inspection of the valve legs
and the holes in the trays show highly polished or worn surfaces.
This is further evidence of high frequency oscillations.   Such
polished surfaces are not seen in normally operating columns;
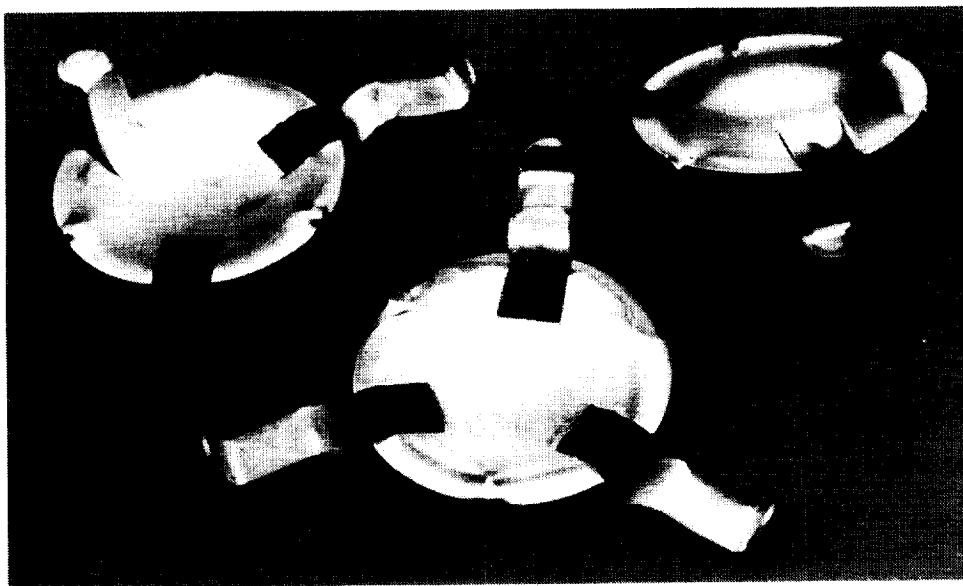i.e., columns that operate in a stable, non-resonant condition.

Figure 9:   Damaged Valves From the Tray Deck

97

Damaged tray hardware shown in Figure 10 includes a small section of a tray deck as well as a damaged and a broken tray attachment clip.
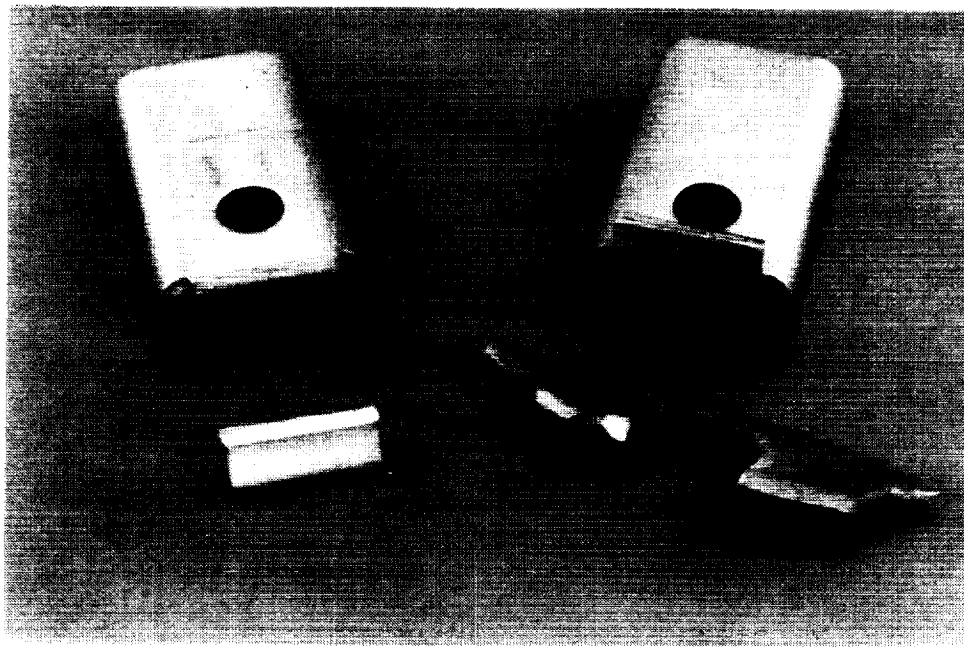
Figure 10: Damaged Tray Hardware
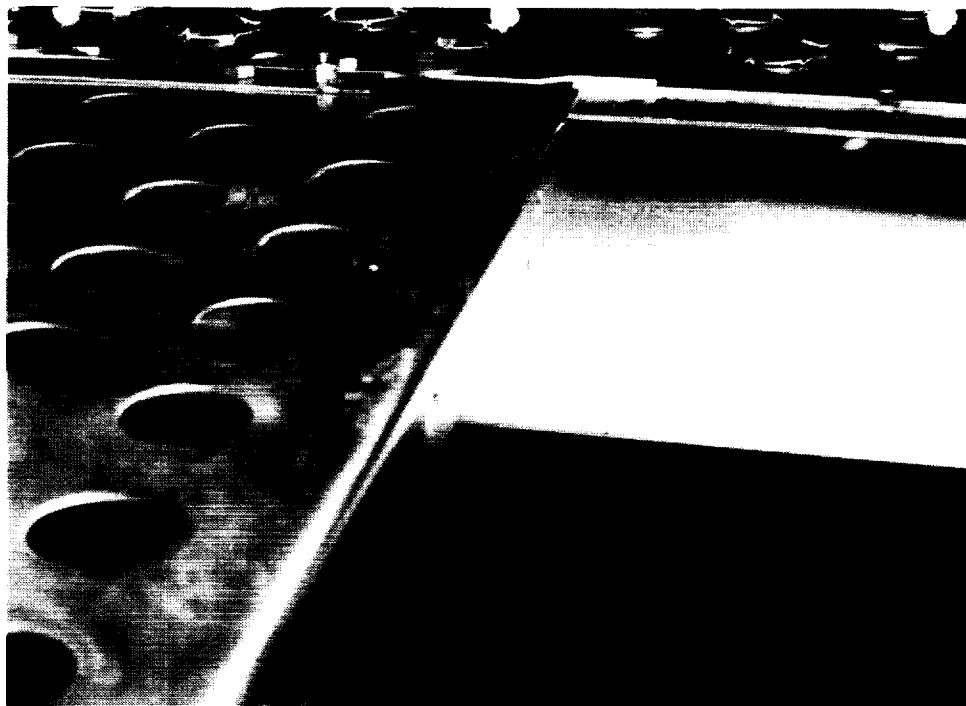
Figure 11: Missing Valves on the Tray Deck
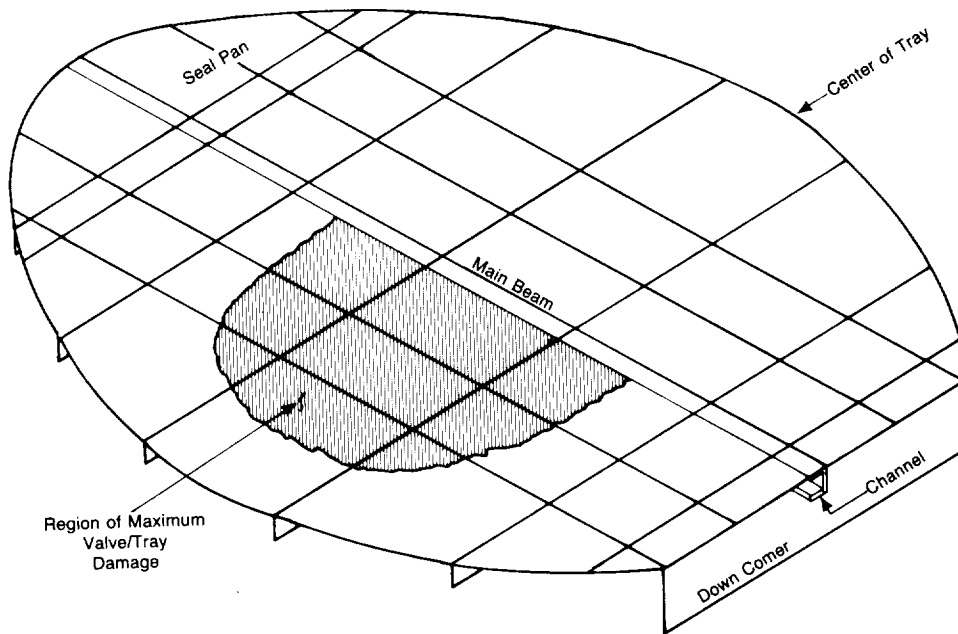
Figure 12: Oblique View of Tray Showing the Region of
Maximum Valve Damage

The missing valves as shown in Figure 11 allow vapor to bypass
the liquid thus decreasing the vapor-liquid interaction and thus
the tray efficiency. This was the first time this type failure
had ever been encountered at the Tennessee Eastman Company. This
was due to two factors: (1) Nearly all columns up to this time
had diameters less than 10 ft., and (2) this tray design was
quite flexible compared to most designs. In any event the tray
manufacturer was contacted to correct the problem.

The vendor recommended some small changes to the minor beams.
Again the cross-flow trays failed during start-up. Subsequently,
they recommended using small stiffeners perpendicular to the
minor beams. The results were the same. By this time a finite
element model had been developed by hand; i.e., hand sketches,
keypunch forms and card decks. This model indicated that the
above structural modifications changed the tray natural frequency
less than 2%. This was definitely not enough to uncouple the
system; i.e., to de-tune it. To appreciably change the first
natural frequency of such a structure requires either a
significant change in stiffness or mass; i.e., a significant
change in the stiffness to mass ratio.

The basic philosophy used to substantially increase the first and
second natural frequencies was to significantly increase the tray
stiffness with only minor increases in mass. By this time it was
obvious TEC was on the cutting edge of tray structural design and
analysis technology. The vendor did not accept our final
recommendations. However, we proceeded with the modifications as
described on the subsequent pages.

Analytical Results

The original model was shown in Figure 6. The first mode is shown in Figure 13. The frequency associated with this mode varies from 16 cps to 18 cps depending on the effective liquid depth on the tray. The mode shape shown in Figure 3 actually looks more like a second mode. However, a careful review of the tray support structure explained the skewed (non-symmetric) shape of this mode. It was due to the use of a channel support beam which resulted in a non-symmetric stiffness distribution relative to the central axis of the tray. If a symmetric beam (I-beam, etc.) located at the center line of the tray had been used then the mode shape would have been symmetric relative to the direction of flow; i.e., about the X axis. Of course the mode would obviously not be symmetric relative to the center of the tray along the Y axis since it is neither stiffness symmetric nor mass symmetric relative to the Y axis; i.e., the Y-Z plane. It is also interesting to note that the ratio of the maximum modal displacements from one side of the main beam to the other is 5.6 to 1. The modal acceleration and thus the inertial loads experienced by the valves also varies by a factor of 5.6 from one side of the main beam to the other; i.e., the forces on the valves are 5.6 times as great in the region opposite the open side of the channel. This would mean valve failures and tray deck damage would occur first and be the most severe on this side of the main beam. This is exactly what visual inspection of the damaged trays had revealed. See Figures 7, 11 and 12.

$\omega_1 = 18$ cps

Notes:
(1) Maximum accelerations/deflection occur between points "a" and "b."
(2) Ratio of modal accelerations between points "a" and "c" is:

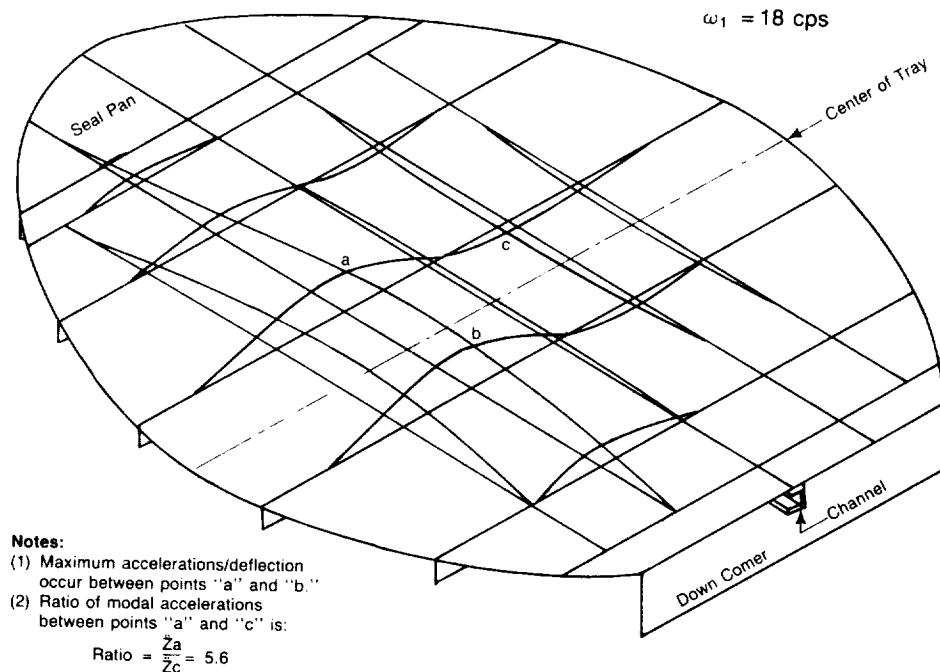$$\text{Ratio} = \frac{Z_a}{Z_c} = 5.6$$

Figure 13: First Mode of the Original Tray Design

Based on these analytical results two structural modifications were investigated. The first consisted of attaching rather large angle stiffeners at two locations perpendicular to the main beam. This increased the first natural frequency substantially; i.e., from 18 cps to 34 cps. This configuration and the first mode shape are shown in Figure 14. As shown in Figure 14, this mode shape is quite symmetric. This is because the combined stiffness of the angles was about the same as that of the channel. However, for process reasons the depth of these angles was such that it would impede the vapor liquid interaction on the tray deck below. Past experience had shown that beams perpendicular to the direction of the liquid flow served to decrease the effective distance between trays (tray spacing) which would decreases the process capacity of the trays.

The next alternative considered involved using smaller angle stiffeners and changing the main beam from a channel to an I-beam. The moment of inertia of the channel was $I_{YY} = 6.29$ in^4 while that of the replacement I-beam was $I_{YY} = 38.25$ in^4. The first natural frequency increased from 16 to 18 cps to 49 cps. The associated mode shape is shown in Figure 15.
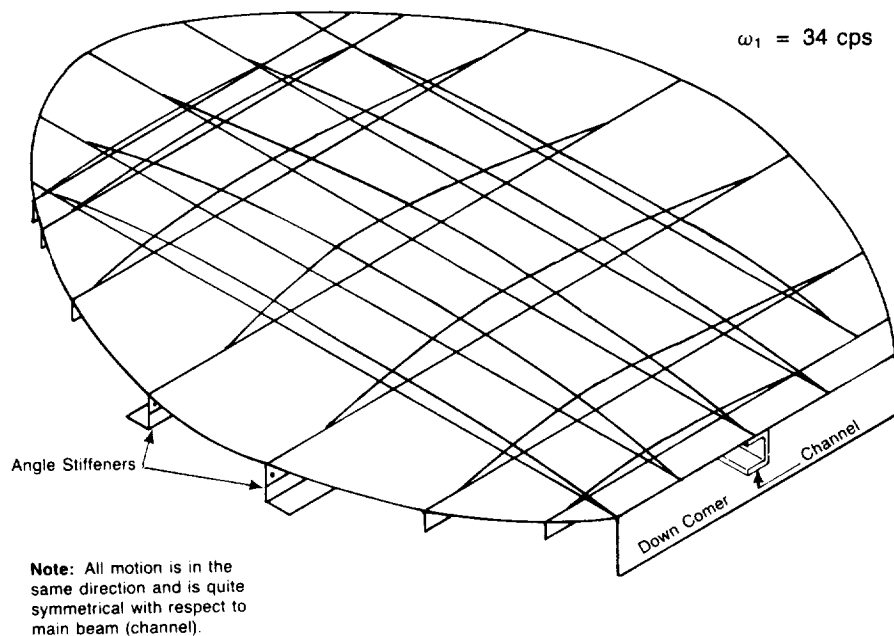

$\omega_1 = 34$ cps

Angle Stiffeners

Down Comer   Channel

Note: All motion is in the same direction and is quite symmetrical with respect to main beam (channel).

Figure 14:   First Mode Shape of Tray Modification A

$\omega_1 = 49$ cps

Angle Stiffeners

Down Comer

"I" Beam

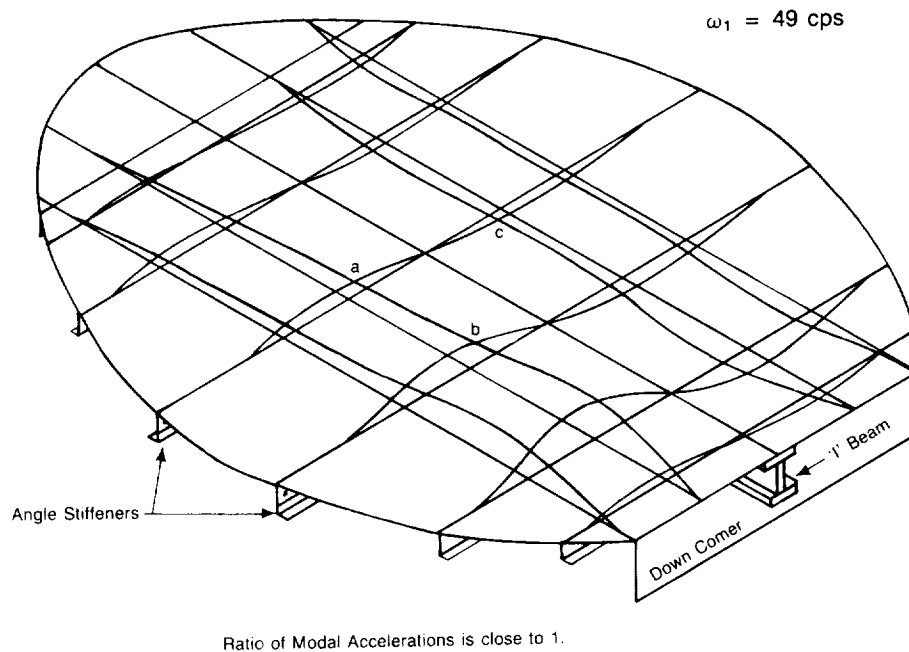Ratio of Modal Accelerations is close to 1.

Figure 15:   First Mode Shape of the Final Modified Tray

The mode shape shown in Figure 15 is still not symmetric even though a symmetric I-beam was used. Again, it looks like a second mode. The reason the first mode is still not symmetric is because the beam had to be set off-center to match-up with existing fastening points on the tray deck. Thus the tray stiffness relative to the X-axis is still not symmetric. At this time, a larger than needed I-beam was used because we did not know the nature of the forcing functions involved. In any event, this corrected the resonant problem.

At a later date, after the structural modifications had been installed, special instrumentation was installed across several trays to measure pressure fluctuations. Depending on the process conditions; i.e., the liquid and vapor flow-rates; the measured process pulsations varied from 16.75 cps to 17.75 cps. This was within the range of the calculated first structural natural frequency range of 16 to 18 cps. Indeed we had a resonance. It had been reported by several persons working near the column that it sounded like a beehive during attempted start-ups; i.e., a very high frequency chatter. In any event, this problem led to the structural parameter study.

102

RESULTS OF THE STRUCTURAL PARAMETER STUDY

The dynamic analysis of various diameter distillation trays shows that the first and second structural natural frequencies decrease with increasing diameter. This result is shown in Figure 16 as a scatter band around the mean values. The scatter band indicates that the natural frequencies vary somewhat depending on the liquid depth; i.e., depends on non-structural mass variations. See Appendix V for additional mode shapes associated with the parameter study.
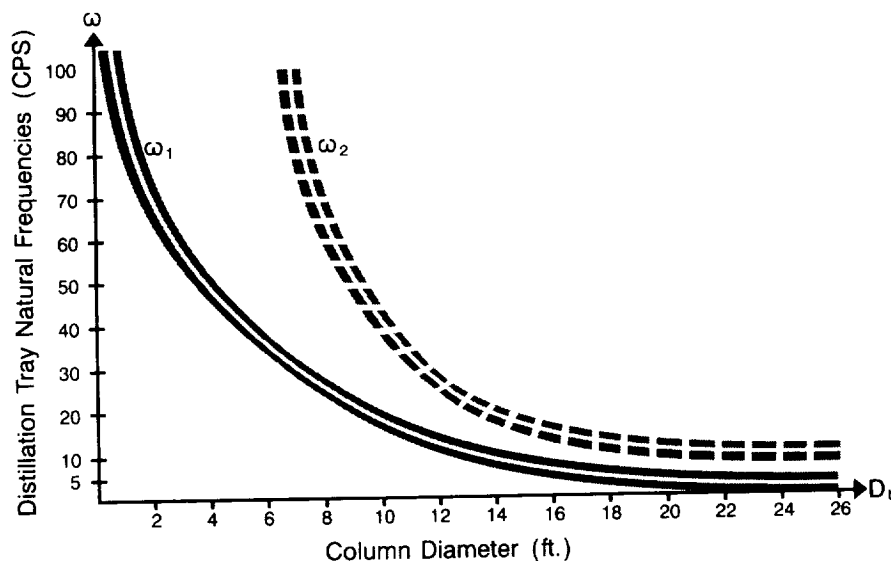

Figure 16: The First and Second Tray Natural Frequencies Versus Tray/Column Diameter

Figures 5 and 16 are combined in Figure 17. It is evident from this figure that at some diameter the frequency of the first or second tray mode has a high probability of coinciding with (being the same as) the auto-pulsation frequency thus producing a resonant condition. Experiences at Tennessee Eastman Company as well as at other petrochemical plants throughout the world agree with this region of maximum incidence of resonance; i.e., at tray diameters between 8 ft. and 16 ft. (2.44 to 4.88 M) for the first mode and 12 ft. to 18 ft. (3.66 to 5.49 M) for the second mode[4]. In-the-field results indicate numerous severe/rapid distillation tray failures have been encountered in this range. However, long term fatigue failures are actually more commonly encountered in this tray diameter range. Fatigue type failures are also very prevalent at tray diameters below and above this diameter range. This is shown in Figure 17. In all diameter ranges corrosion has been a problem which in many cases has been stress corrosion cracking (SCC). One must be aware that SCC failures often mimic fatigue failures. Thus, one should always have a metallurgical analysis performed when tray cracking is observed to determine if the culprit is truly fatigue or stress corrosion cracking or a combination of SCC and fatigue.
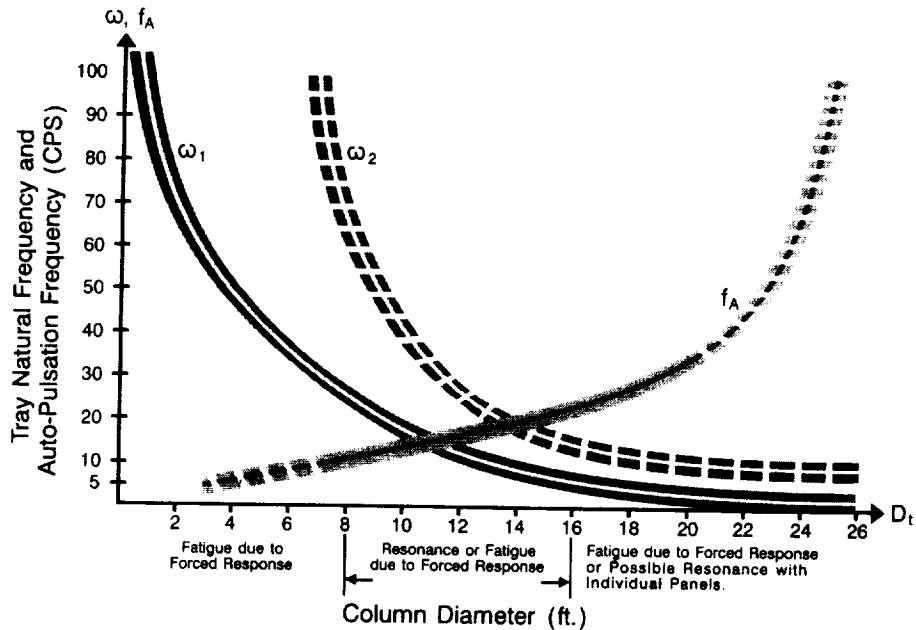
ω, f_A

Tray Natural Frequency and
Auto-Pulsation Frequency (CPS)

100
90
80
70
60
50
40
30
20
10
5

ω₁   ω₂

f_A

2 4 6 8 10 12 14 16 18 20 22 24 26   D_t

Fatigue due to
Forced Response

Resonance or Fatigue
due to Forced Response

Fatigue due to Forced Response
or Possible Resonance with
Individual Panels.

Column Diameter (ft.)

Figure 17:   Graphs of the First and Second Tray Natural
Frequencies and the Auto-Pulsation Frequency
Versus Tray/Column Diameter

In an effort to determine the sensitivity of the distillation
tray's dynamic and static response to the various structural
parameters studied, a regression analysis using all of the
analytical data was performed. The resulting polynomial
equations are shown in Appendix IV. These correlations can be
used for "rough" estimates of a trays first and second natural
frequencies and static deflection. They should only be used to
determine if a thorough finite element analysis is needed. As a
rule of thumb I would recommend that a dynamic analysis be
performed or the tray structure changed if the first or second
natural frequency predicted by these relationships is within 8 to
10 cps of a suspected process or auto-pulsation frequency.

The first tray natural frequency correlation in the 10 ft. to 12
ft. diameter range shows that diameter has the largest effect
with the main beam having the next largest effect. The next most
influential parameters are the minor beam with liquid level being
the least influential. This simply indicates that the easiest
way to substantially change the first tray natural frequency, ω_1,
is to modify stiffness of the the main beam. The second would be
by changing the stiffness of the the minor beams.

In the same diameter range, the second natural frequency is again
most sensitive to tray diameter but the second and third
parameters are the minor beams and the liquid depth. The main
beam is not a factor because it acts as a nodal line or neutral
line for the second mode. Modifying the minor beams is the best
way to change the second natural frequency, ω_2.

104

In the 12 ft. to 15 ft. range, again diameter is the most influential parameter on the first tray natural frequency, ω_1. Next is the main beam. In this diameter range the liquid level has a much greater effect. The minor beam effects are relatively insignificant since this parameter, I_C, does not show up in the relationship. Again, the most effective way to change the first natural frequency is to modify the main beam, I_B.

As in the previous situation, the second natural frequency, ω_2, is most sensitive to diameter with the minor beams and liquid depth being the next most significant parameters. As expected the major beam has very little effect. Thus modifications of the minor beams is the most effective way to change the second tray natural frequency in the 12 ft. to 15 ft. range.

A similar correlation for static deflection in the 10 to 12 feet range shows diameter has the largest affect followed by the main beams and minor beams. Of course, to reduce the tray deflection at any given diameter one would increase the stiffness of either or both the main beam and/or minor beams.

A special correlation indicating the percent of the total tray load carried by the main beam is also presented. As one would expect increasing the stiffness of the minor beams reduces the percent load carried by the main beam since this serves to transmit more of the load to the support ring which is welded to the vessel wall. Thus increasing the stiffness of the minor beams serves to reduce the relatively high loads that exist where the main beam attaches to the vessel wall.

Discussion of Other Type Tray Structural Failures

As indicated previously, longer term fatigue failures are a more common mode of tray failure. This is indicated at the bottom of Figure 17. In many processes the action on the tray decks is quite violent; i.e., there are large pressure variations across the trays. Fortunately this usually does not result in a resonant condition. Instead, the tray is subjected to forced response which leads to long term fatigue failures. Examples of such failures are shown in Figures 18 and 19. An indication of the violent action and resulting large deflections is shown in Figure 20. Note that there are washers in the cracks between tray panels. These washers could not be pulled out. They were wedged in the cracks between tray panels. This indicates the presence of large tray deflections. Of course all of the hardware laying on the tray deck was shaken loose from the above trays by the violent pulsations existing in this particular column. Fortunately, many distillation trays operate in relatively mundane environments and never experience such failures.

In the diameter range greater than 15 feet, trusses are generally used for structural support. See Appendices I, II and III. In the diameter range exceeding 20 feet, two tray decks may be

supported from the same truss or trusses. In this diameter range, a possible resonant condition with a portion of a tray is possible. However, again, the most likely failure mode is fatigue with corrosion often being a problem.
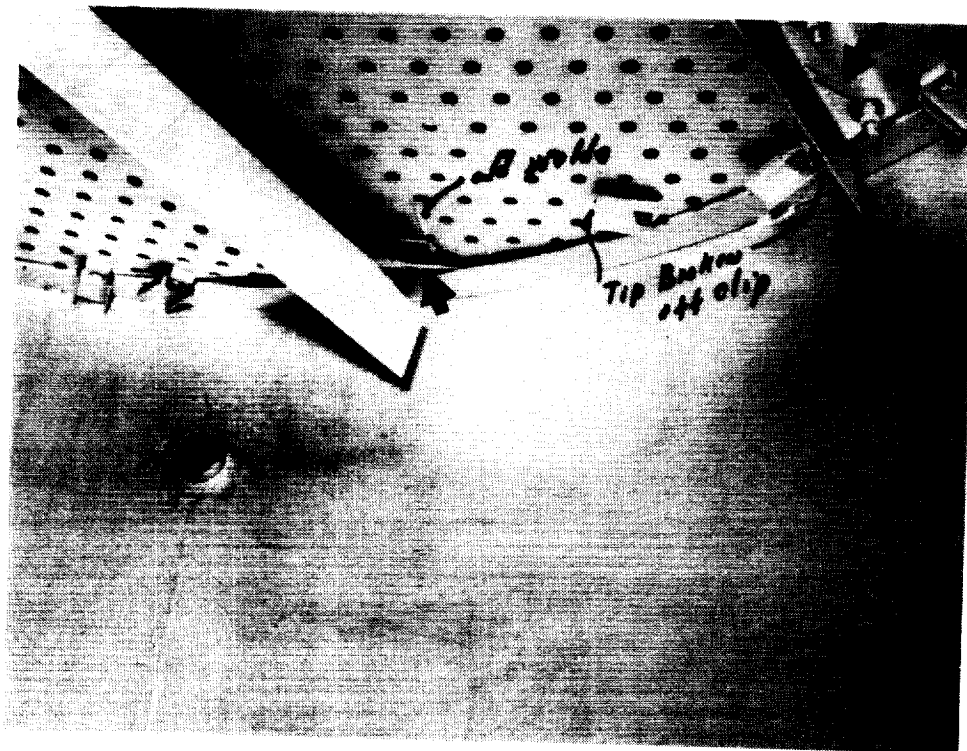

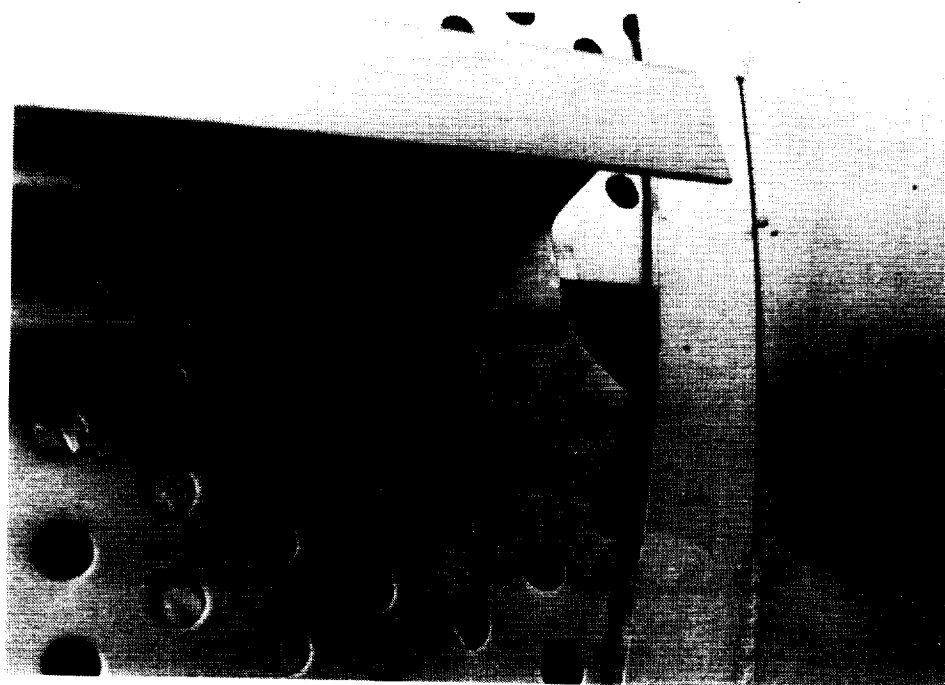Figure 18: Typical Tray Fatigue Failure (Severe)
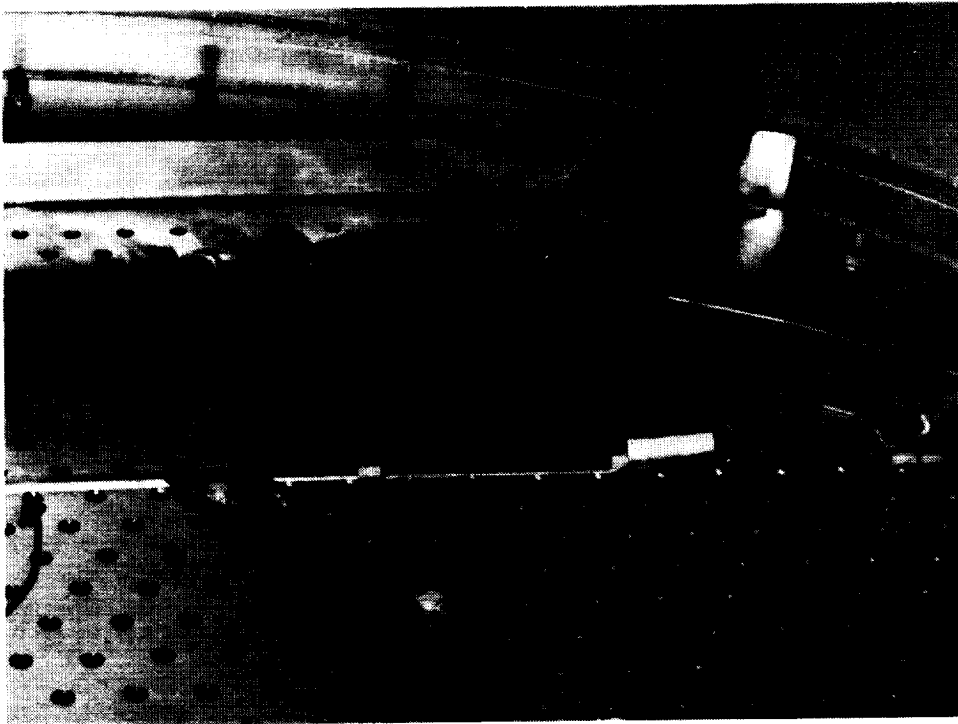

Figure 19: Typical Tray Fatigue Failure (Local)

Figure 20: Evidence of Large Tray Deflections

It should be noted that a marginal tray design from a dynamic point of view can encounter a resonant condition after several years of operation if it experiences sufficient corrosion to reduce the first or second natural frequency to the range of the auto-pulsation frequency. This has been encountered at Tennessee Eastman Company. This is another reason you would prefer to have at least a 10 cps difference between the first tray natural frequency, ω_1, and any suspected process pulsation or auto-pulsation frequency. This is especially important if you may have corrosion problems; i.e., if you have specified a corrosion allowance.

Another, unfortunately too frequent failure mode is associated with sudden and severe over-pressure of the trays. Since trays are usually designed for a static load (pressure drop) of 25 to 45 psf (0.17 to 0.31 psi) a relatively small pressure pulse can blow the trays out. Such pressure pulses are generally associated with the rapid vaporization or flashing of a pool of liquid at the base of the column or near a process feedstream, a minor internal explosion or a sudden loss of vacuum. Such conditions usually occur during a process upset or during start-up or shut-down of the process. Some typical damage from such situations is shown in Figures 21 and 22.

Figure 21:   Tray Damage Due to Flashing in the Base of a Column
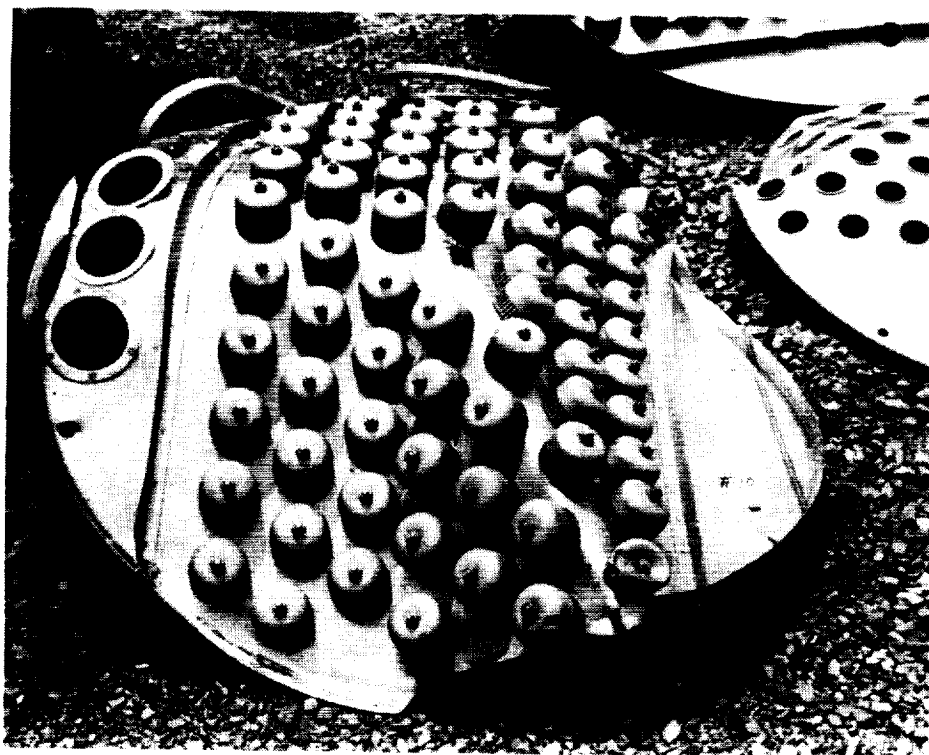   (10 ft. diameter)

Figure 22:   Severe Over-pressure of a Bubble-Cap Tray
             (5 ft. Diameter)

108

Certain sections of a column are more susceptible to such damage than others. As a result we generally increase the design load for the trays in these regions; i.e., use a design load of 90 to 130 psf. It is important to realize that the tray panels are designed such that they will come apart when subjected to a large over pressure; i.e., they serve as a pressure relief mechanism. If this was not done, then the over pressure would have to be absorbed by the vessel wall. This would in many cases rip a hole in the vessel wall. To prevent such occurrences would require much thicker vessel walls along with special reenforcements where main beams are attached to the vessel. This would substantially increase the cost of such units and adversely affect product costs. It should also be realized that the tray panels, as designed, are quite flexible and can easily be repositioned. For instance, the seemingly severe damage shown in Figure 21 was repaired within a few weeks; i.e., the trays were reassembled with very few new parts being required.

Conclusions:

This structural parameter study has shown that cross flow distillation trays in the 10 to 15 feet diameter range are susceptible to resonant conditions. It has further identified which structural parameters can be most effectively used to correct a resonant condition and reduce fatigue damage. In addition, these results can be used to prepare static design specifications that reflect dynamic requirements. This is important since many distillation tray vendors at this time do not have the capability to perform the dynamic analysis and thus cannot comply with dynamic specifications.

A future study, Phase II, will extend this cross flow distillation tray structural parameter study to a diameter range of 3 feet to 10 feet.

REFERENCES

(1) NASTRAN Users Manual (NASA SP-222), COSMIC, Barrows Hall, University of Georgia, Athens, Georgia 30601

(2) NASTRAN Programmers Manual (NASA SP-223), COSMIC, Barrows Hall, University of Georgia, Athens, Georgia 30601

(3) Priestman, G. H.; Brown, D. J.: "The Mechanism of Pressure Pulsations in Sieve Tray Columns", Institute of Chemical Engineers, Dept. of Chemical Engineering & Fuel Technology, Sheffield University, England, Trans I ChemE, Vol. 59, 1981.

(4) Priestman, G.H.; Brown, D. J.; Kohler, H. K.; "Pressure Pulsations In Sieve-Tray Columns", ICHEM.E. Symposium Series No. 56.

(5) Biddulph, M. W.; Stephens, D. J.; "Oscillating Behavior on Distillation Trays," Dept. of Chemical Engineering, University of Nottingham, University Park, England.

(6) Brierley, RJP; Whyman, PJM; Erskine, JB; "Flow Induced Vibration of Distillation and Absorption Column Trays", Imperial Chemical Industries Limited, I. Chem. E. Symposium, Series No. 56.

LIST OF APPENDICES

I. Typical Valve Trays

II. Typical Sieve Trays

III. Large Diameter Trays and Other Tray Configurations

IV. Regression Analysis of Analytical Results

V. Some Typical Mode Shapes

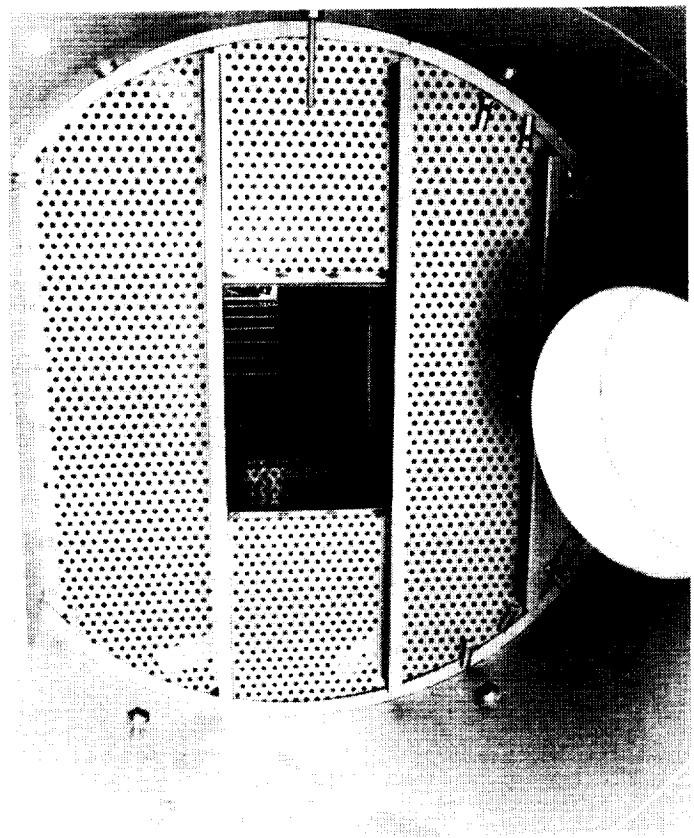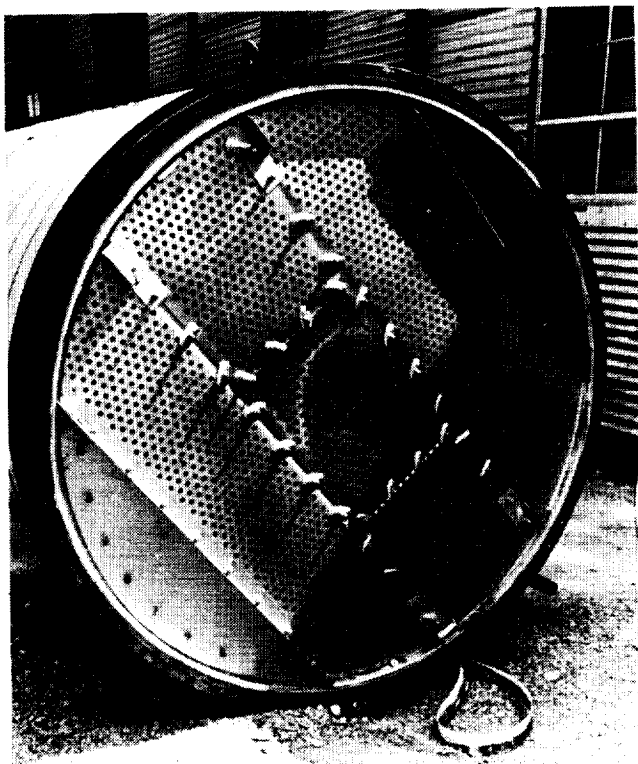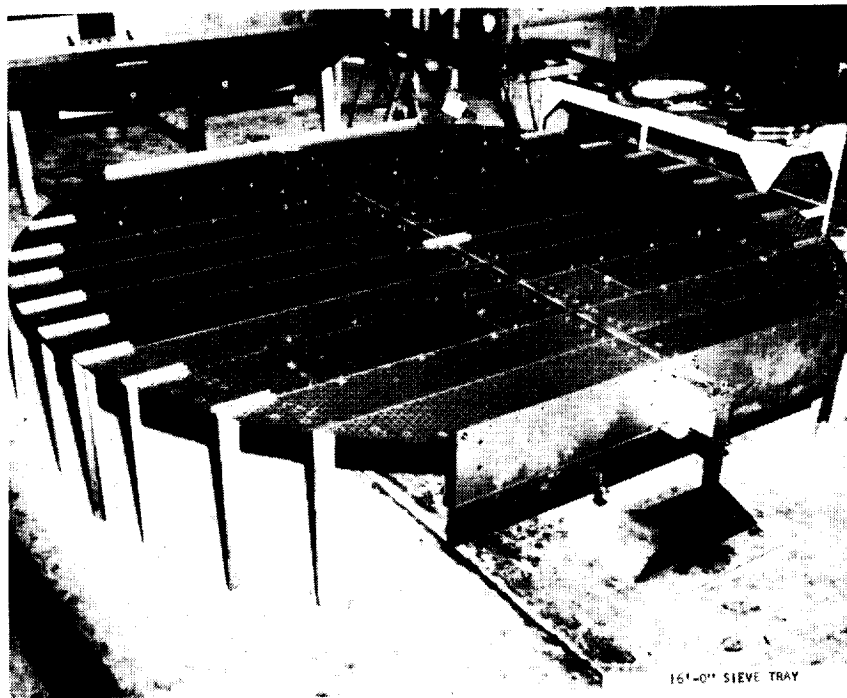VI. Typical Boundary Conditions and an Example Static Load Set

TYPICAL VALVE TRAYS
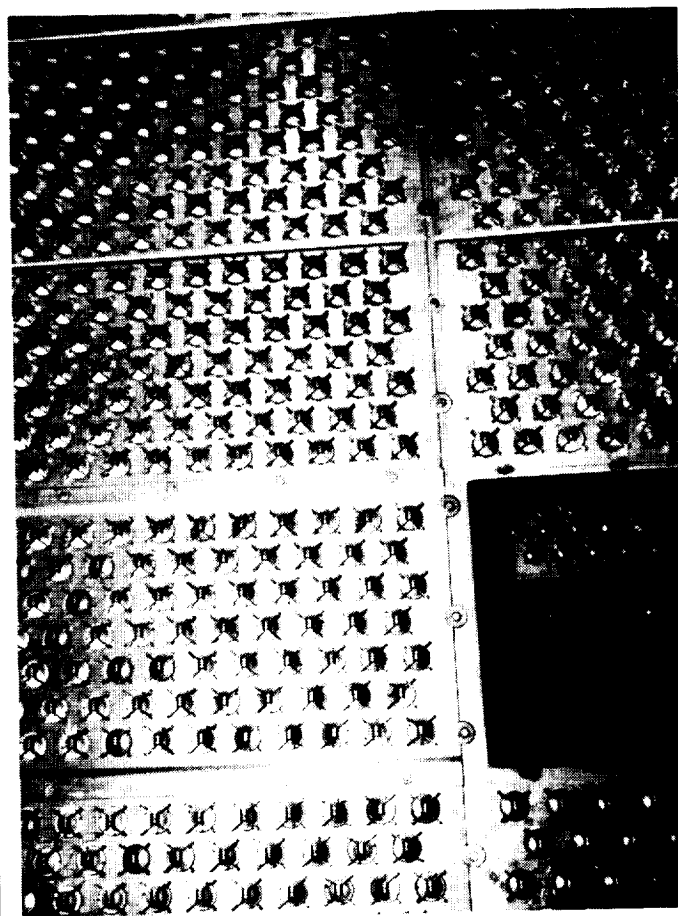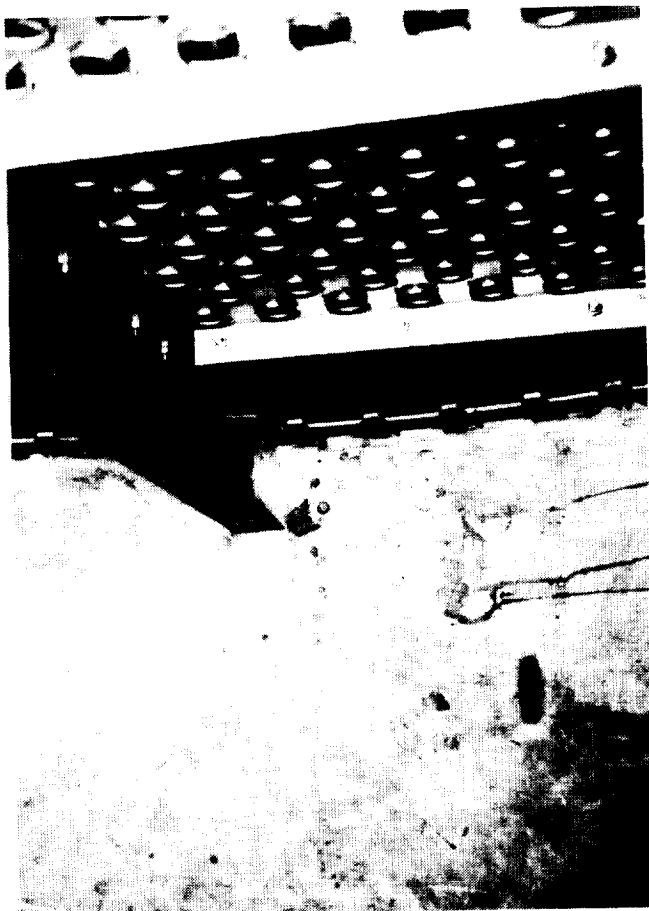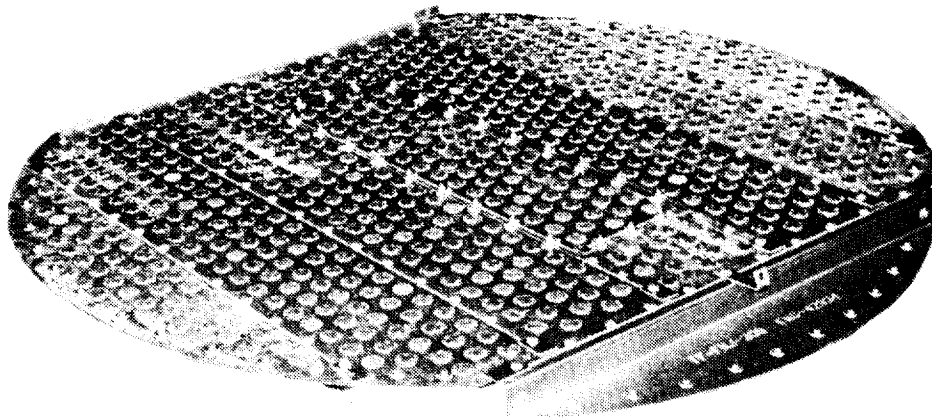
See Appendix III for Large Diameter Distillation Trays.
(D_t > 16 ft.)

ORIGINAL PAGE
BLACK AND WHITE PHOTOGRAPH

ENGINEERING DRAWING OF A TYPICAL VALVE TRAYS

SECTION "A-A"

½" HIGH DEFLECTOR WEIR

MANWAY

5'-0" I.D. TOWER

APPENDIX II

TYPICAL SIEVE TRAYS

16'-0" SIEVE TRAY

ORIGINAL PAGE
BLACK AND WHITE PHOTOGRAPH

LARGE DIAMETER TRAYS AND OTHER TRAY CONFIGURATIONS

22'-0" 4-PASS VALVE TRAY

114
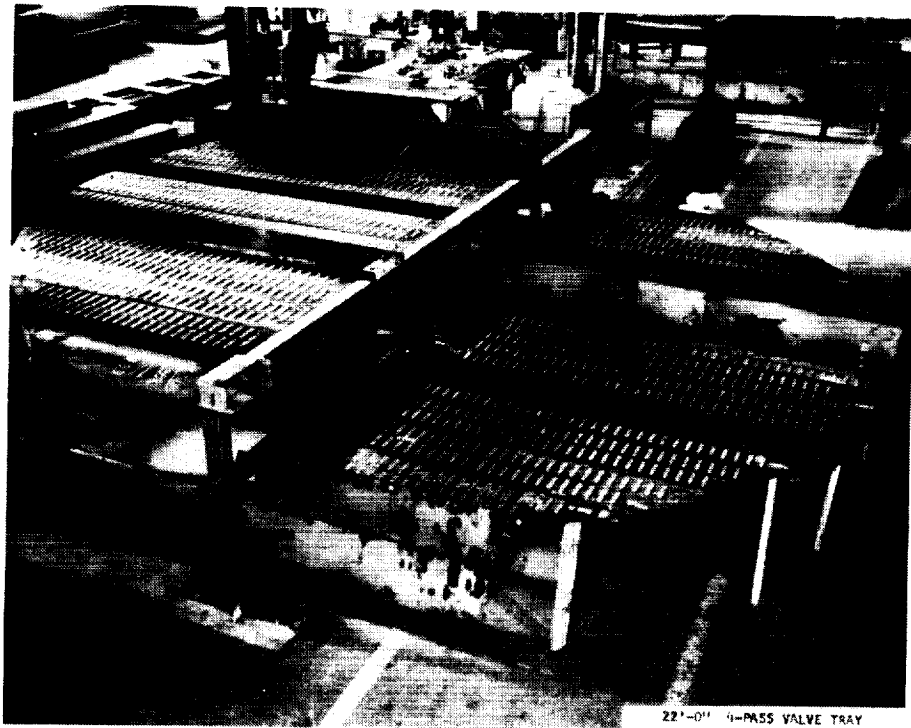
LARGE DIAMETER TRAYS AND OTHER TRAY CONFIGURATIONS
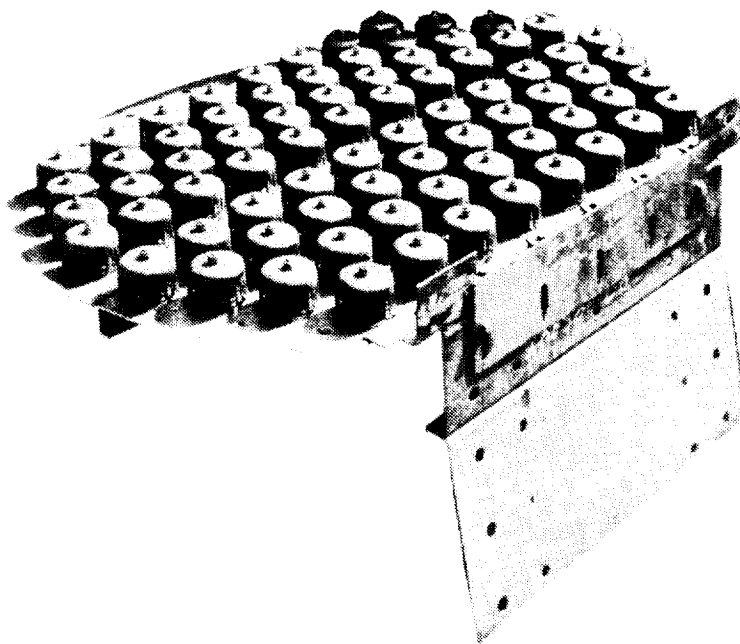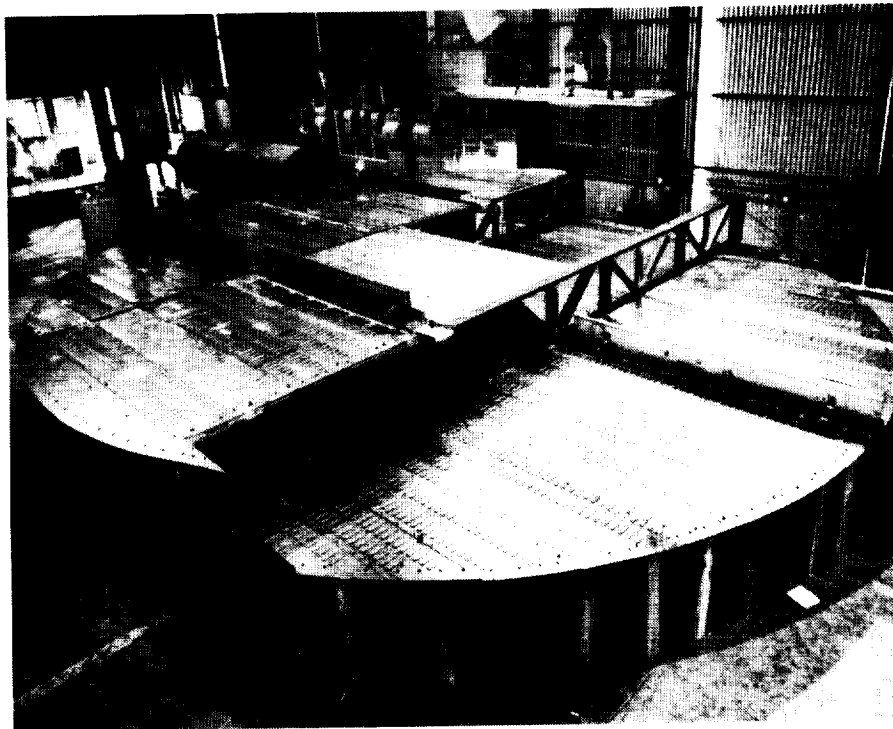
Smaller Diameter Bubble Cap Tray

APPENDIX IV

RESULTS OF THE REGRESSION ANALYSIS OF THE ANALYTICAL RESULTS

NOTE: (1) $I_S = \Sigma I_{Si}$ (In.^{4})

(2) I_{Si} = Moment of Inertia of the Small Beams (In.^{4})

(3) D_t = Tray Diameter in Feet

(4) I_B = Moment of Inertia of Main Beam (In.^{4})

(5) h_L = Liquid Depth in the Active Area (Ins.)

FOR ESTIMATING FIRST AND SECOND NATURAL FREQUENCIES (ω_1, ω_2), [cps]

12' > D_t > 10'

$$\omega_1 \simeq 51.6332 - 3.927 D_t + .6236\,I_S + 1.6068\,I_B - .0196\,I_S^2 - .512\,I_B h_L$$

$$\omega_2 \simeq 117.416 - 7.334 D_t + 3.674\,I_S + 8.733\,h_L - .0847\,I_S^2$$

15' > D_t > 12'

$$\omega_1 \simeq 49.947 - 3.0419 D_t + .6098\,I_B - 3.3942\,h_L - .0075\,I_B^2$$

$$\omega_2 \simeq 109.26 - 6.656 D_t + 3.709\,I_S - 8.386\,h_L - .088\,I_S^2$$

FOR ESTIMATING THE DEFLECTION DUE TO A UNIFORM STATIC LOAD OF 35 PSF/64 PSF (INS.)

12' > D_t > 10'

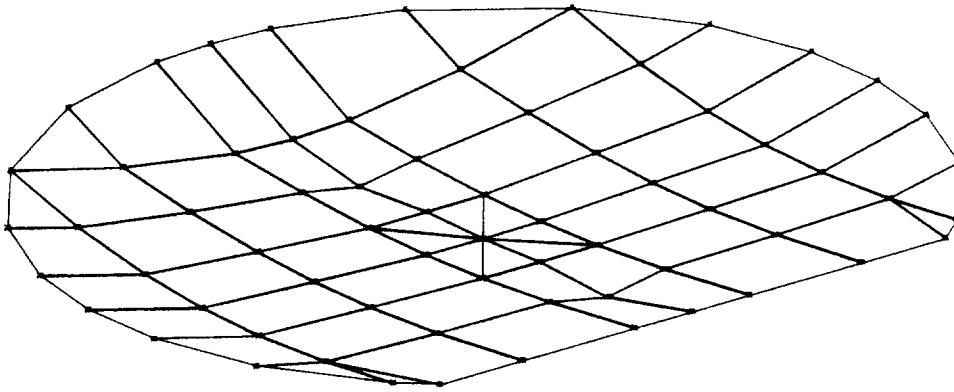$$\delta_Z \simeq -.1348 + .0327 D_t - .0088\,I_S - .0057\,I_B + .00025\,I_S I_B$$

FOR ESTIMATING PERCENT LOAD CARRIED BY THE MAIN BEAM
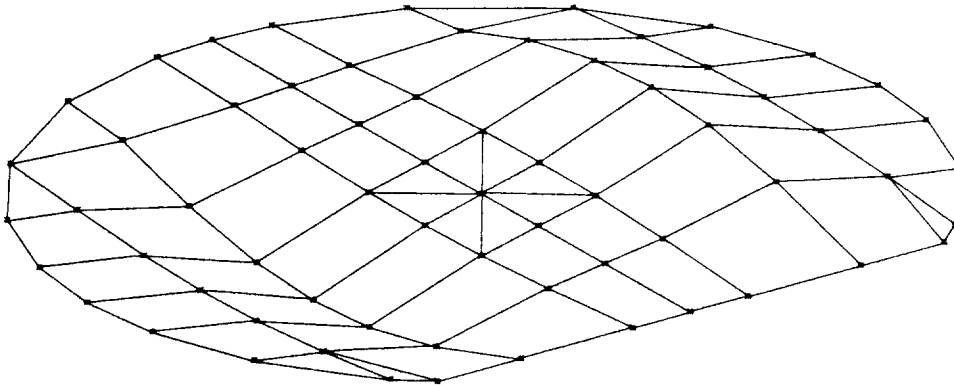
12' > D_t > 10'

$$\%F_B \simeq 51.78 - 2.1162\,I_S + .8379\,I_B - .0199\,I_B^2 + .0512\,I_S I_B$$
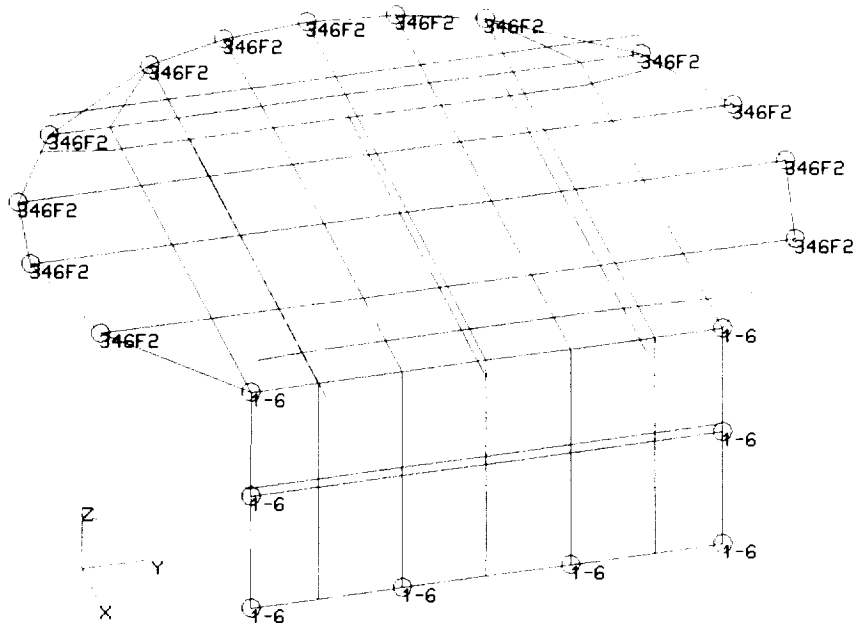
116

SOME TYPICAL MODE SHAPES

First Mode Shape

Second Mode Shape
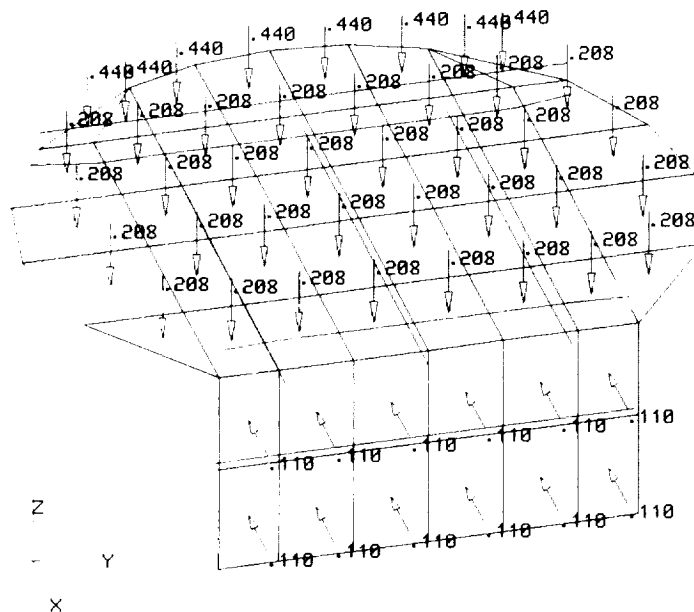
117

APPENDIX VI

TYPICAL BOUNDARY CONDITIONS

NOTE:

$123\ 456 = XYZ\ R_X\ R_Y\ R_Z$ or RO $R_R\ R_O\ R_Z$

346F2 means Z $R_R\ R_Z$ are constrained (Cord. 2)

1-6 means XYZ $R_X\ R_Y\ R_Z$ are constrained

EXAMPLE STATIC LOAD SET

Note: Loads are in psi [0.208 psi = 30 psf, 0.440 psi = 64 psf, 0.110 psi = 16 psf].